

Observed transitions in $n = 2$ ground-state configurations of copper, nickel, iron, chromium, and germanium in tokamak discharges

E. Hinnov, S. Suckewer, S. Cohen, and K. Sato*

Princeton University, Plasma Physics Laboratory, Princeton, New Jersey 08544

(Received 22 October 1981)

A number of spectrum lines of highly ionized copper, nickel, iron, chromium, and germanium have been observed and the corresponding transitions identified. The element under study is introduced into the discharge of the Princeton Large Torus tokamak by means of rapid ablation by a laser pulse. The ionization state is generally distinguishable from the time behavior of the emitted light. New identifications of transitions are based on predicted wavelengths (from isoelectronic extrapolations and other data) and on approximate expected intensities. All the transitions pertain to the ground-state configurations of the respective ions, which are the only states strongly populated at tokamak plasma conditions. These lines are expected to be useful for spectroscopic plasma diagnostics in the 1–3-keV temperature range, and they provide direct measurement of intersystem energy separations from chromium through copper in the oxygen, nitrogen, and carbon isoelectronic sequences.

INTRODUCTION

The various ionization stages of any element that may be present in a tokamak discharge exhibit a space and time behavior that is partly determined by atomic properties, i.e., ionization and recombination rates, and partly by the characteristics of the plasma, e.g., electron temperature, density distribution, and radial particle transport rates. This characteristic allows on the one hand utilization of appropriate emission lines for localized spectroscopic plasma diagnostics, and on the other hand it is helpful for identifying any previously unknown lines and atomic transitions.

In the Princeton Large Torus PLT tokamak¹ during the quasisteady phase of an ohmically heated discharge, the central electron temperatures are usually in the range $T_e(0) \approx 1.5 - 2$ keV, but in special cases $T_e(0) \approx 3 - 4$ keV may be reached. The observed maxima of radial distributions of particular ionization states, e.g., of iron, are in most cases located about radii such that $T_e(r) \approx E_i$, the ionization potential of the state, i.e., at significantly higher temperatures than the corresponding coronal ionization equilibrium maxima.^{2,3} The perceived deviations from equilibrium are thought to be caused primarily by radial particle transport and therefore could be used to measure such rates.

However, quantitative attempts of such transport measurements have foundered in the past, partly on the uncertainties of the ionization^{4,5} and recombination^{6,7} rates and partly on insufficiently detailed data on the ion radial distributions.

The uncertainties in the atomic rates could be eliminated to a large extent, or at least evaluated, by measuring the distributions of the ions of two or more elements simultaneously. This would allow quantitative comparison of, e.g., the behavior of Cr XXII, Fe XXII, Ni XXI, and Cu XXI—all with $E_i \approx 1.7 - 1.8$ keV but quite different electronic structure and hence atomic rates—under the same plasma conditions [$T_e(r), n_e(r)$, etc.]. At different radii, i.e., different temperatures, an analogous set of appropriate ions would be measured.

Traditionally, the ion densities are measured from space-resolved absolute emissivities of their resonance lines. This is particularly appropriate in the case of ions of ns and ns^2 ground configurations, which have very strong and relatively well-established (wavelengths, transition probabilities) resonance lines. However, in the more complicated configurations it is often difficult to find appropriately isolated resonance lines, considering that several neighboring elements are to be present in the plasma, and therefore not only is the spectrum fairly crowded, but also the concentration of each

element must be severely limited in order to avoid significant radiative energy losses. In typical tokamak plasmas the total allowable density limit for medium Z ($\sim 20-30$) elements is about $5 \times 10^{10}/\text{cm}^3$ or $\sim 10^{-3}n_e$.

In this respect magnetic dipole lines within the ground configurations of such ions offer many diagnostic advantages^{8,9} that derive mostly from their relatively long wavelengths. Aside from their application for ion density measurements these lines are also eminently useful for measurements of local ion temperatures¹⁰ and plasma rotations,¹¹ and other spatially localized phenomena^{12,13} in tokamak plasmas.

In order to extend the available data base of suitable magnetic dipole lines, to allow greater choice of diagnostic wavelengths, and particularly to increase the applicable electron temperature range [related to the ions by the $E_i \sim T_e(r)$ condition] a systematic search for such lines has been undertaken in the PLT tokamak. In the present paper we report the results for the $2s^22p^x$ configurations in copper and nickel, many additions and some revisions in iron and chromium, and the establishment or improvement of accuracy of wavelengths of several other lines of diagnostic interest in tokamaks and similar plasmas.

A parallel and complementary part of this program is the development and refinement of the technique of introducing the desired elements into the discharge in predetermined amounts and appropriate times. The method used in this work is the sudden ablation of a metal film by a ruby laser pulse,^{14,15} also called the laser blowoff method. The technical details of applying this procedure to large, high-temperature tokamaks will be discussed elsewhere,¹⁶ but we shall describe some aspects of it that have direct influence on the wavelength measurements and other spectroscopic diagnostic applications.

EXPERIMENTAL

With a few exceptions most of the line wavelengths and intensities discussed in this paper were measured or remeasured by means of the laser blowoff injection of the element. The target plasmas included a considerable variety of ohmically heated discharges, because most of the wavelength-identification measurements were performed in plasmas devoted to other, unrelated experiments requiring different conditions. However, in most cases the electron densities in the measure-

ment region were not very far from $3 \times 10^{13} \text{ cm}^{-3}$, and the peak temperatures along the line of sight were 1.5–2.5 keV. For some of the copper measurements the necessary higher temperatures, ~ 3 keV, were reached adding some neon to the discharge. Neon, by radiative cooling of the plasma periphery, produces a more centrally peaked current-density and temperature profile. Unfortunately it also adds to the radiation (straylight) problems and often exhibits lines of its own precisely at the wavelengths to be measured. Carbon (originating primarily from the graphite aperture limiter) and oxygen lines are always present to some extent, and the discharge also contained small intrinsic amounts of Ti, Fe, Cr, and Ni.

The element to be injected is deposited on a glass plate, facing the plasma, and is illuminated from behind by an about 1 J ruby laser pulse. The ablated material is partly vapor and partly small (0.2–5- μ -diam) globules, which become evaporated and ionized in the outer layers of the target plasma. The amount of injected material is of the order of 10^{17} atoms per shot ($\sim 2-3 \times 10^{10}/\text{cm}^3$ if spread uniformly over the plasma volume), and this amount may be varied by adjusting the laser focus or the thickness of the deposit. For initial search of unidentified lines, somewhat (2–3 \times) larger amounts were often used to facilitate distinction from background radiation. It appears feasible to inject several elements simultaneously in predetermined ratios by this method, although at present actual tokamak experience in this regard is meager.

The injection generally occurs at a time when the target plasma is in a quasisteady state for at least 100–200 ms. On the time scale of the subsequent behavior of the higher ionization states of the injected element, the injection is practically instantaneous, the emitted radiation time behavior being determined by subsequent toroidal and radial transport and by the rates of ionization and recombination. The atomic rates, ionization and recombination, are, of course, implicitly dependent of the radial transport, since the latter determines the local electron temperature and density.

The line intensities were measured with two spectrometers located toroidally nearly opposite, or about 300 cm, from the injection port. The instrument for $\lambda \leq 1200 \text{ \AA}$ is a 1-m 85° incidence bichromator, with a 2400 groove/mm holographic grating, and magnetic electron multipliers with tungsten photocathodes for detectors. The measured instrumental profile is a near-Gaussian with

half-intensity width 0.82 \AA in the first order for the higher-wavelength channel, and 1.10 \AA for the other. The wavelengths were measured, after the approximate location was determined, by advancing the exit slit by usually $\frac{1}{4} \text{ \AA}$ increments shot by shot, with the other channel monitoring some other already known line of the injected element for reproducibility. The wavelength scale is established by interpolation from known carbon, oxygen, and iron lines. The estimated (first-order) wavelength accuracy is about $\pm 0.2 \text{ \AA}$, somewhat better in most favorable cases (strong lines, with no significant interference from other lines and not very far from reference wavelengths) and perhaps $\pm 0.3 \text{ \AA}$ in weaker lines, subject to interference.

At $\lambda \geq 1400 \text{ \AA}$ the wavelengths were measured with a 1-m helium or argon filled Ebert-Fastie monochromator with external LiF optics. This instrument is generally used in fourth–eighth order, mostly for Doppler width measurements. Although it has a good spectral resolution the absolute wavelength accuracy is limited by the interpolations from known wavelengths and varies again from about $\pm 0.1 \text{ \AA}$ to about $\pm 0.3 \text{ \AA}$, depending on conditions.

Both instruments are calibrated for absolute intensity measurements against NBS standard lamps and arcs at longer wavelengths, and by radiative branching ratios at shorter wavelengths. The sensitivity of the Ebert system deteriorates rapidly below $\sim 1400 \text{ \AA}$, and the sensitivity of the grazing incidence spectrometer deteriorates above $\sim 1100 \text{ \AA}$, thus there are no measurements of relatively weak lines in this interval.

Above $\lambda = 2000 \text{ \AA}$ a third monochromator, a $\frac{1}{2} = m$ Ebert-Fastie equipped with a rotating mirror system for spatial scanning as well as a vibrating mirror for rapid spectral scans, was used for initial wavelength location and radial emissivity distribution measurements of lines in this spectral region.

Figure 1 illustrates some of the measurement problems as well as advantages of the laser injection method. Copper was injected into the PLT discharge (with neon) at about 495 ms, i.e., when the discharge had already lasted for about 0.5 s and had a central $T_e(0)$ about 3.1 keV, $n_e(0)$ about $3 \times 10^{13} \text{ cm}^{-3}$. The figure shows time behavior of three copper ion lines, normalized to their maxima: a Cu XXI ($E_i = 1.79 \text{ keV}$) magnetic dipole line, a Cu XXIV ($E_i = 2.17 \text{ keV}$) magnetic dipole line, and the Cu XXVI ($E_i = 2.46 \text{ keV}$) singlet resonance line. The Cu XXI and XXVI lines are from the same

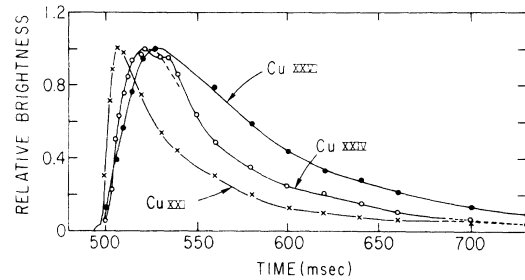


FIG. 1. Time behavior of observed brightness of three copper lines after injection (495 ms): Cu XXI $\lambda = 592.3 \text{ \AA}$, Cu XXIV $\lambda = 756.9 \text{ \AA}$, and Cu XXVI $\lambda = 111.2 \text{ \AA}$.

discharge, measured by the two spectrometer channels, while the Cu XXIV line is from a different discharge when both the target plasma and the amount of copper may have been slightly different.

The ordinates are line brightnesses measured in the equatorial plane with background signal (continuum emission, straylight, etc., measured without copper injection subtracted). Although the ordinate scales are known (peak values were 4×10^{13} , 8×10^{13} , and $9 \times 10^{14} \text{ photons/cm}^2 \text{ s sr}$ for the Cu XXI, XXIV, XXVI lines, respectively), the intensities are not directly comparable as they correspond to different spatial distributions along the line of sight. These, together with many other data of plasma diagnostic interest will be discussed in a subsequent paper. Only the lines of a given ionization state have sufficiently similar spatial distributions for direct quantitative comparisons of chord brightnesses. However, we note that the ionization times for these three ions near the center of the discharge are about 0.5, 1.0, and 3.0 ms, respectively, i.e., the time (and space) variations must be largely determined by ion transport, except that the difference between the risetime of Cu XXIV and XXVI may be significantly affected by ionization times. The structure near the peak of the Cu XXIV line appears to be caused by some transient plasma phenomenon. In the same discharge as the others it probably would have appeared as indicated with the dotted curve.

The time shapes of the line intensities are often sufficiently distinct to allow unambiguous assignment of a newly observed line to the proper ionization state, and of course the right element is *a priori* specified by injection. This is a great advantage over spontaneously occurring elements in the discharge, where such assignment is frequently pre-

carious. However, even with injection there are problems, especially in the case of weaker lines and earlier states of ionization, where time differences between adjacent states are small. Often many measurements at different plasma conditions (especially peak temperatures) and including radial distributions are necessary for proper identification.

One type of problem is illustrated in Fig. 1 by the 111.2 Å line of Cu XXVI. This is a very strong line (indeed the strongest line in the copper spectrum—provided the temperature is sufficient, ≥ 2.5 keV, to easily reach the berylliumlike state) and there is no doubt about the identity near the peak (in time and space). However, it clearly begins to rise before the Cu XXIV line (and Cu XXV) and it also extends further in radial extent. Precisely the same behavior has been observed in the isoelectronic $2s^2 1S-2s 2p^1 P$ line in iron,¹⁷ and it is ascribed to a nearly exact coincidence (within ~ 0.1 Å) with the $2s^2 2p^3 4S_{3/2}-2s 2p^4 4P_{5/2}$ transition—of Cu XXIII in this case. At lower temperatures the latter line is of course progressively relatively stronger.

Another and more pervasive problem is illustrated by the small initial shoulder on the Cu XXI line in Fig. 1 and in Fig. 2. The latter shows two Cu XXIV lines ascribed to the $2s^2 2p^2 3P_1-3P_0$ and $1D_2-3P_1$ transitions at 756.9 and 540.0 Å, respectively. The signal at the second line has a substantial early peak which clearly does not belong to Cu XXIV.

Such early signals are very prevalent. Their precise origin is not established except that it is radiation and is associated with the injected element. It varies, both in intensity and in time behavior, with wavelength setting (hence, it is not primarily straylight) becoming generally stronger at shorter wavelengths (which may mean that straylight is a non-negligible component; indeed observations with a crystal spectrometer at around the *L*-line wavelengths of the injected element also exhibit such early signals with characteristics expected of straylight).¹⁸ Apparently it becomes stronger with heavier elements. From the early appearance and evidently peripheral space distribution the origin of this radiation must be the lower states of ionization, e.g., Cu I—XIX.

In the present case Fig. 2 shows the signal at three wavelength settings: at the peak of the 540 Å line, and 1.5 Å either side, normalized to the peak values. At either side the radiation is very small after 18–20 ms (not necessarily zero, but too small to distinguish from background and also small compared to the signal at 540 Å). Assuming

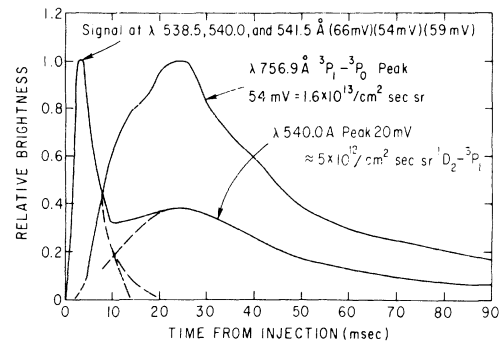


FIG. 2. Appearance of interfering radiation, ascribed to earlier states of ionization of copper, in the neighborhood of the $\lambda = 540.0$ Å intercombination line of Cu XXIV, $2s^2 2p^2$ configuration.

that the interfering signal has the same shape at 540 Å it leaves a signal that is very similar to the 757 Å line (it also has the proper radial width and a reasonable intensity for the assigned transition). Thus in this case the assignment is reasonably secure. However, if the interfering signal had a noticeable lingering plateau (as it often does at other wavelengths) and if it were still larger relative to the sought line, the identification would clearly become dubious or impossible. A special case of this problem arises when a resonance line of an earlier ionization state (even in second or third order, in the case of strong lines) falls very near the wavelength of a weak line being sought. Such cases apparently occur in iron (Fe XX and XXI) spectra as will be mentioned later.

Still another problem arises from the presence of intrinsic impurity lines in the discharge, e.g., oxygen or carbon. Although the intensity time behavior usually allows distinction of the injected element line, the presence of a strong and wavelength-dependent background radiation deteriorates the achievable precision.

Because of this multitude of measurement problems and plasma conditions, it cannot be readily predicted which lines are most useful for plasma diagnostics under given circumstances except in the general sense that brighter lines and longer wavelengths (which in itself is a conflicting requirement) are desirable. The objective of the program, even from the most utilitarian viewpoint, must be to establish systematic trends and sequences in wavelengths and transition probabilities. The variety of conditions encountered in the measurements also explains why some lines are easily measured and confidently assigned to particular

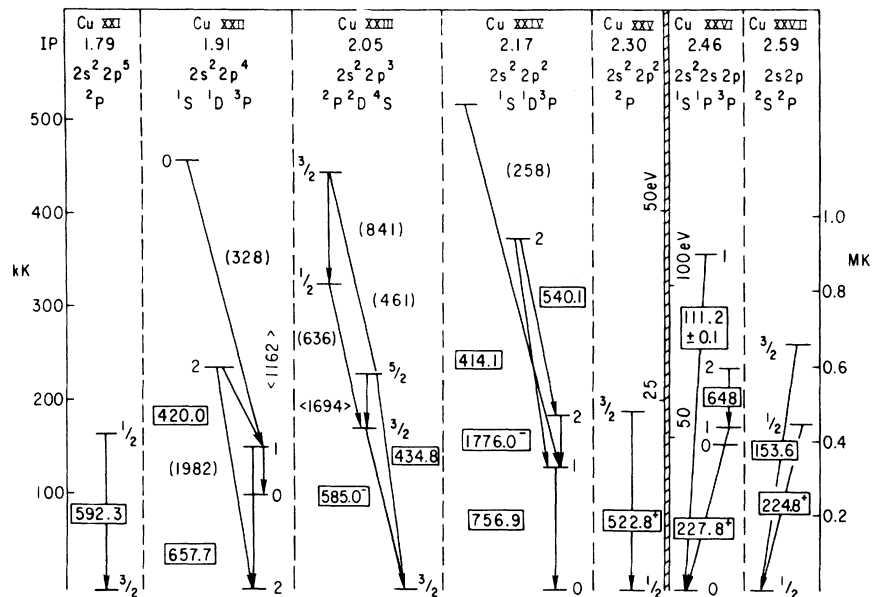


FIG. 3. The $2s^2 2p^x$ ground configurations and the $2s-2p$, $2s^2-2s 2p$ transitions in copper. Observed wavelengths in boxes. Ionization potentials indicate approximate temperature of maximum emissivity in tokamak discharges.

TABLE I. Magnetic dipole lines of $n=2$ configurations. Wavelengths $> 2000 \text{ \AA}$ are given in air. Numbers in parentheses are deduced from measured level differences.

	Cr	Fe	Ni	Cu	Ge
$2s^2 2p^5$					
$^2P_{1/2} \rightarrow ^2P_{3/2}$	1410.6	974.8 +	694.5 +	592.3 -	379.6 +
$2s^2 2p^4$					
$^3P_1 \rightarrow ^3P_2$	1656.3	1118.2	779.5 +	657.7	410.7
$^3P_1 \rightarrow ^3P_0$			2818.2		
$^1D_2 \rightarrow ^3P_2$	740.8	592.2	471.3	420.0	
$^1D_2 \rightarrow ^3P_1$	(1340.2)	(1259)	(1192)	(1162)	
$^1S_0 \rightarrow ^3P_1$	493.8				
$2s^2 2p^3$					
$^2D_{3/2} \rightarrow ^4S_{3/2}$	793.3		634.8	585.0 -	427.9
$^2D_{5/2} \rightarrow ^4S_{3/2}$	(663)		477.6	434.8 -	
$^2D_{5/2} \rightarrow ^2D_{3/2}$	4039	2665.0 -	(1929)	< 1694 >	
$2s^2 2p^2$					
$^3P_1 \rightarrow ^3P_0$	2090.9	[1354.1]	911.0 -	756.9	454.8 -
$^3P_2 \rightarrow ^3P_1$	2885.4	2298.0	1915.0	1776.0 -	1470
$^1D_2 \rightarrow ^3P_2$	979.0	786.1	614.8 -	540.0 +	
$^1D_2 \rightarrow ^3P_1$	731.1 -	585.8 -	465.4	414.1	
$^1S_0 \rightarrow ^3P_1$	398.4				
$2s^2 2p$					
$^2P_{3/2} \rightarrow ^2P_{1/2}$	1205.9	845.5 +	609.9 +	522.8 +	
$2s 2p$					
$^3P_2 \rightarrow ^3P_1$		1079.3		648.0	

transitions while others, superficially similar transitions, may require repeated measurements and modifications.

RESULTS

The measured wavelengths of the $n = 2$ shell magnetic dipole lines are listed in Table I, and the energy levels and transition for copper are shown in Fig. 3. The wavelengths in boxes (Fig. 3) have been observed in the PLT tokamak, as described above. The + and - signs on some wavelengths indicate that the actual value is probably slightly ($< 0.1 \text{ \AA}$) above or below the number given. Wavelengths given in parentheses are predicted values by Edlén.^{19,20}

Aside from previously published scandium²¹ and titanium^{22,23} lines, Table I lists all the $n = 2$ magnetic dipole lines, in elements from chromium to germanium, measured to date in the PLT tokamak discharges, including several that have been reported before.^{22,24}

In the fluorine sequence $2s^2 2p^5$, only copper and germanium lines have not been reported before. Note that the copper wavelength practically coincides with the Fe XIX $2s^2 2p^4 \ ^1D_2 - ^3P_2$ line.

In the oxygen sequence, $2s^2 2p^4 \ ^3P_1 - ^3P_2$, the nickel, copper, and germanium lines are new observations. They are all fairly prominent lines in tokamak discharges, although the nickel line suffers some interference from O IV. In the $^3P_1 - ^3P_0$ only the nickel line has been seen so far. At $Z \leq 25$ this transition is very weak (infrared), but at higher Z it could be of plasma diagnostic interest.

The $^1D_2 - ^3P_2$ intercombination transitions were all strong and easily identifiable by their resemblance to the $^3P_1 - ^3P_2$ time shape. However, the $^1D_2 - ^3P_1$ transitions have not been observed partly because of the above-mentioned instrument sensitivity problem and partly because this transition is inherently rather weak, as the radiative branching ratio favors strongly the other component. Nevertheless, this series may be of special interest because it tends to retain a fairly long wavelength with increasing Z .

In the $^1S_0 - ^3P_1$ sequence only the Cr XVII 493.8- \AA line has been seen so far. In nickel ($\sim 359 \text{ \AA}$) and copper ($\sim 328 \text{ \AA}$) the search has been hampered by the high level of interfering background radiation, and not very much work has been done in PLT with iron injection because the iron spec-

trum is already relatively well known. This transition will probably be readily observable in scandium, titanium, and vanadium.

In the nitrogen sequence $2s^2 2p^3$, the Fe XX, $^2D_{5/2} - ^2D_{3/2}$ 2665- \AA line was the first magnetic dipole transition applied to tokamak diagnostics, but the $^2D_{5/2,3/2} - ^4S_{3/2}$ have not been found. The first of these appears to nearly coincide with the second order of the strong Fe XV resonance line (284.15 \AA), and the second similarly with the Fe XVI resonance line (360.80 \AA). However, both of these transitions have been readily located in nickel and copper, thus also establishing the $^2D_{5/2} - ^2D_{3/2}$ wavelengths. In nickel this transition at $\sim 1929 \text{ \AA}$ apparently was observed directly (while searching another line) but its wavelength has not yet been adequately measured. Another somewhat cursory observation of the $^2D_{5/2} - ^2D_{3/2}$ line at $\sim 4039 \text{ \AA}$ in chromium, together with the definitely established 793.3- \AA , $^2D_{3/2} - ^4S_{3/2}$ line, predicts the $^2D_{5/2} - ^4S_{3/2}$ line of chromium just below 663 \AA . In Ge XXVI the $^2D_{3/2} - ^2S_{3/2}$ line at 427.9 \AA was readily measured, but the other component suffered from strong interfering radiation (with time-shape corresponding roughly to Ge XXI). This line (Ge XXVI, $^2D_{5/2} - ^4S_{3/2}$) is tentatively located at 319.2 \AA (which would put the $^2D_{5/2} - ^2D_{3/2}$ line $\sim 1257 \text{ \AA}$), but this requires further confirmation.

In the carbon sequence $2s^2 2p^2$, as has been already reported,²⁴ two previously misassigned transitions have been corrected: the $^3P_1 - ^3P_0$ at 2090.9 \AA in Cr XIX, and the $^3P_2 - ^3P_1$ at 2298.0 in Fe XXI. The latter, although a fairly strong line, is difficult to observe because of its proximity to a very strong C III line. The Fe XXI line at 1354 \AA is established from solar flare observations.^{25,26} We have not seen it in tokamak discharges because of our spectrometer sensitivity problem. The $^3P_2 \rightarrow ^3P_1$ sequence in this configuration is of particular interest for tokamak diagnostics, as it retains relatively long wavelengths to high- Z elements; but, unlike the $^1D_2 - ^3P_1$ in oxygen sequence, it has no adverse radiative branching to reduce its intensity. The 1470 \AA line of Ge XXVII in this sequence is still a preliminary measurement and may have to be revised slightly in the future. As in the case of oxygen sequence, none of the $^1S_0 - ^3P_1$ transitions have been reliably observed beyond Cr XIX. In Fe XXI the expected wavelength¹⁹ coincides with a Fe XVI resonance line, and in Ni and Cu the background radiation has been too high, although in copper a suggestion of a line with proper time behavior has been seen just below 258 \AA .

In boron sequence the $2s^2 2p^2 P_{3/2} \rightarrow ^2P_{1/2}$ in the Ni XXIV and Cu XXV are new observations. The former suffers from interference with oxygen lines, and its wavelength may be actually closer to 610.0 Å than to 609.9 Å.

In beryllium sequence we have observed the $2s 2p^3 P_2 \rightarrow ^3P_1$ line in Cu XXVI, at 648.0 Å. This transition has been seen²³ in Sc XVIII (2907.9 Å), Ti XIX (2344.6 Å),^{22,27} and Fe XXIII (1079.3 Å),²² and it undoubtedly will be observable in Cr, Ni, etc., as well. Aside from its high-temperature diagnostic interest ($E_i = 2.46$ keV in Cu XXVI), the intensities of these lines in conjunction with the corresponding singlet resonance lines and $^3P_1 - ^1S_0$ intercombination lines may elucidate some of the excitation rate problems in berylliumlike configurations.

Aside from the lines listed in Table I, we have also measured the following wavelength of other transitions of diagnostic interest:

Cu XIII	$3s^2 3p^5 ^2P_{1/2} - ^2P_{3/2}$	3500.4 Å
Cu XVII	$3s^2 3p^2 P_{3/2} - ^2P_{1/2}$	3007.6 Å
Cu XXVI	$2s 2p^1 P_1 - 2s^2 ^1S_0$	111.2 Å
Cu XXVI	$2s 2p^3 P_1 - 2s^2 ^1S_0$	227.8 + Å
Cu XXVII	$2p^2 P_{3/2} - 2s^2 S_{1/2}$	153.6 Å
Cu XXVII	$2p^2 P_{1/2} - 2s^2 S_{1/2}$	224.8 + Å
Ge XXI	$3s 3p^1 P - 3s^2 ^1S_0$	196.60 Å
Ge XXII	$3p^2 P_{3/2} - 3s^2 S_{1/2}$	226.50 Å

The last two were measured in third order and have an estimated accuracy of ± 0.05 Å. We have also improved a previously reported²² wavelength measurement in Ti XIX ($2s 2p^1 P \rightarrow 2s^2 ^1S$) to 169.58 ± 0.02 Å.

The Cu XXVI resonance line problem was mentioned in the preceding section. It has been observed in the fifth order, where the intrinsic wavelength accuracy is about 0.04 Å, but the intensity is weak. There do appear to be two copper lines, one between 111.1–111.2, the other between 111.2–111.3 Å. From time behavior the second seems to be the Cu XXVI line. However, further measurements at different plasma temperatures are necessary to clarify this.

The assignment of the 227.8 Å line to Cu XXVI should also be regarded as somewhat tentative. If a nearby ionization state (e.g., Cu XXV or XXIV) has a strong resonance line at 113.9 Å, its second order could mask or distort this measurement.

Finally, we want to make some remarks about the intensities and, in particular, representative intensity ratios of the various lines in a given ioniza-

tion state. Several such ratios are given in Table II. We stress that the different ions are not quantitatively comparable, as they correspond to different experimental conditions. Also, the absolute magnitudes are only a rough guide of what may be expected in a tokamak-type plasma, with the elements in question present in sufficient amounts for various diagnostics. The corresponding strongest electric-dipole resonance lines of these ions would have intensities of the order $10^{14}/\text{cm}^2 \text{ s sr}$, i.e., a few hundred in the scale of Table II. We note that the stronger magnetic dipole lines are within a factor 10 of this figure and that the intercombination lines are typically about 2–3 times weaker than the transitions within the ground term. Such estimates are likely to be useful in future search for similar transitions.

Radiative transition probabilities for all $n=2$ ground configurations up to zinc ($Z=30$) and also several heavier elements have been calculated by Cheng, Kim, and Desclaux.²⁸ The accuracy of these presumably can be improved by scaling them to the experimental wavelengths. The observed intensities are, of course, primarily determined by collisional transition rates and therefore do not necessarily have any simple relationship to the radiative rate. However, the intensity ratios of lines originating on a common upper level, e.g., $^1D_2 \rightarrow ^3P_2, ^3P_1$, or $^2D_{5/2} \rightarrow ^2D_{3/2}, ^2S_{3/2}$, are strictly determined by radiative rates, and their precision in branching ratios is important; such line ratios are eminently useful for improving the intensity calibration of the spectrometers. If the sensitivity at one of the wavelengths is known, measuring the response of the other component establishes the sensitivity at its wavelength. This is of substantial practical importance in the range ~ 300 – 500 Å and also ~ 600 – 900 Å, where there is a dearth of suitable calibration lines.¹⁷

TABLE II. Approximate intensities of various transitions.

Ion	Wavelengths (Å)	Intensities $10^{12}/\text{cm}^2 \text{ s sr}$
Cu XXIV	757:414:540	23:10:8
Ni XXII	635:478	25:18
Cr XIX	398:731:979	8:6:9
Cr XVII	494:741	6:14

We have not attempted any detailed comparisons with previous work. Direct observations of the magnetic dipole lines of these elements appear to have been made only for iron in solar flares.^{25,26} Energy levels from resonance-line measurement in chromium, iron, and nickel have been recently obtained by Lawson and Peacock²⁹ from laser-produced plasmas and by Breton³⁰ *et al.* from TFR tokamak discharges. Transition rates in chromium, iron, and nickel ions have been discussed by Feldman *et al.*³¹ in a paper that also reviews available energy-level data. A recent comprehensive listing, including observations of titanium ions in Dite tokamak, is given by Lawson, Peacock, and Stamp.²⁷ Older literature is summarized in the NBS energy level compilations.³²⁻³⁴ Copper and germanium spectra in fluorine and oxygen sequences have been observed by Behring *et al.*,²⁵ and by Kononov *et al.*,³⁶ and are discussed in the compilation of Edlén.²⁰ A cursory examination of these data where they overlap our measurements show generally good agreement, but it also shows several instances of significant discrepancies.

SUMMARY

We have established by direct wavelength measurements most of the $2s^2 2p^x$ energy levels in copper and nickel, as well as the 1D levels in iron and $^1D, ^1S$ levels in chromium, for $x = 2, 4$. The principal exceptions are the 1S levels (except chromium), where interfering background radiation

was too intense, and some of the nitrogen sequence levels, where the search has not been completed. Also several other lines in copper and germanium ions have been measured. Some of the wavelength measurements notably the $\lambda \sim 4039 \text{ \AA}$ and $\lambda \sim 1929 \text{ \AA}$ lines in nitrogenlike chromium and nickel, respectively, the $\lambda \sim 1470$ line in Ge XXVII, and the berylliumlike copper, $\lambda = 111.2$ and $\lambda = 227.8$ lines, require further improvement and confirmation. All these lines are of potential or actual interest in local spectroscopic diagnostics of tokamak-type plasmas in the 1–3-keV electron temperature range. Some of the line pairs originating from a common initial level are also important for improving spectrometer sensitivity calibration in the far UV.

ACKNOWLEDGMENTS

The authors wish to thank the PLT tokamak operators and other physicists attempting to conduct their own disparate experiments for their forbearance, especially on the rare occasions where a too enthusiastic injection led to an untimely disruption of a discharge. The authors are also indebted to Dennis Manos and John Timberlake for able assistance with the injection procedures. Various communications and comments by Professor Bengt Edlén have been very helpful in the identification of the forbidden transitions. This work has been supported by United States Department of Energy under Contract No. DE-AC02-76-CHO-3073.

*Visitor from Nagoya University, Institute for Plasma Physics.

¹K. Bol *et al.*, *Plasma Physics and Controlled Nuclear Fusion Research*, Proceedings of the 7th International Conference, Innsbruck, 1978 (IAEA, Vienna, 1979), Vol. I, p. 1.

²S. Suckewer and E. Hinnov, *Phys. Rev. A* **20**, 578, (1979).

³E. Hinnov, *Atomic and Molecular Processes in Controlled Thermonuclear Fusion*, edited by M. R. C. McDowell and A. M. Ferendeci (Plenum, New York, 1980), p. 449.

⁴D. H. Crandall, R. A. Phaneut, B. E. Hasselquist, and D. C. Gregory, *J. Phys. B* **12**, L249 (1979).

⁵P. Greve, M. Kato, H. J. Kunze, and R. S. Hornady, *Phys. Rev. A* **24**, 429 (1981).

⁶A. L. Merts, R. D. Cowan, and N. H. Magee, Jr., LASL Report No. LA-6220-MS (unpublished).

⁷Y. Hahn, *Phys. Rev. A* **22**, 2896 (1980).

⁸S. Suckewer and E. Hinnov, *Phys. Rev. Lett.* **41**, 756 (1978).

⁹E. Hinnov, R. Fonck, and S. Suckewer, *Bull. Am. Phys. Soc.* **25**, 690 (1980); also Princeton Report No. PPPL-1669 (unpublished).

¹⁰H. Eubank *et al.*, *Phys. Rev. Lett.* **43**, 270 (1979).

¹¹S. Suckewer, H. Eubank, R. Goldston, E. Hinnov, and N. Sauthoff, *Phys. Rev. Lett.* **43**, 207 (1979).

¹²E. Hinnov *et al.*, *Bull. Am. Phys. Soc.* **25**, 902 (1980).

¹³S. Suckewer, E. Hinnov, M. Bitter, R. Hulse, and D. Post, *Phys. Rev. A* **22**, 795 (1980).

¹⁴S. Cohen, J. Cecchi, and E. Marmar, *Phys. Rev. Lett.* **35**, 1507 (1975).

- ¹⁵E. Marmor, J. Cecchi, and S. Cohen, *Rev. Sci. Instrum.* **46**, 1149 (1975).
- ¹⁶D. Manos, D. Ruzic, R. Moore, and S. Cohen, *J. Vac. Sci. Tech.* (in press).
- ¹⁷E. Hinnov, in *Diagnostics for Fusion Experiments*, edited by E. Sindoni and C. Wharton (Pergamon, Oxford, England, 1979), p. 139.
- ¹⁸S. von Goeler, private communication, 1981.
- ¹⁹B. Eldén, private communications, 1981.
- ²⁰B. Eldén, *Phys. Scr.* **22**, 593 (1980).
- ²¹S. Suckewer, J. Cecchi, S. Cohen, R. Fonck, and E. Hinnov, *Phys. Lett.* **80A**, 259 (1980).
- ²²E. Hinnov and S. Suckewer, *Phys. Lett.* **79A** 298 (1980).
- ²³S. Suckewer, R. Fonck, and E. Hinnov, *Phys. Rev. A* **21**, 924 (1980); **22**, 2278 (1980).
- ²⁴S. Suckewer and E. Hinnov, in the Proceedings of the XII International Conference on the Physics of Electron and Atomic Collisions, Gatlinburg, Tennessee, 1981 (unpublished).
- ²⁵G. A. Doschek *et al.*, *Astrophys. J.* **196**, L83 (1975).
- ²⁶G. D. Sandlin, G. E. Brueckner, and R. Tousey, *Astrophys. J.* **214**, 898 (1977).
- ²⁷D. K. Lawson, N. J. Peacock, and M. F. Stamp, *J. Phys. B* **14**, 1929 (1981).
- ²⁸K. T. Cheng, Y. K. Kim, and J. P. Desclaux, *At. Data Nucl. Data Tables* **24**, 111 (1979).
- ²⁹K. D. Lawson and N. J. Peacock, *J. Phys. B* **13**, 3313 (1980).
- ³⁰C. Breton, C. DeMichelis, M. Finkenthal, and M. Mattioli, *J. Opt. Soc. Am.* **69**, 1652 (1979).
- ³¹U. Feldman, G. A. Doschek, C. C. Cheng, and A. K. Bhatia, *J. Appl. Phys.* **51**, 190 (1980).
- ³²J. Sugar and C. Corliss, *J. Phys. Chem. Ref. Data* **6**, 317 (1977).
- ³³J. Reader and J. Sugar, *J. Phys. Chem. Ref. Data* **4**, 353 (1975).
- ³⁴C. Corliss and J. Sugar, *J. Phys. Chem. Ref. Data* **10**, 197 (1981).
- ³⁵W. E. Behring, L. Cohen, G. A. Doschek, and U. Feldman, *J. Opt. Soc. Am.* **66**, 376 (1976).
- ³⁶E. Ya. Kononov, A. N. Rybatseu, U. I. Safranova, and S. S. Churilov, *J. Phys. B.* **9**, L477 (1976).